Carbohydrate Polymers 80 (2010) 525–532

Contents lists available at ScienceDirect

Carbohydrate Polymers

journal homepage: www.elsevier.com/locate/carbpol

Preparation and properties of biodegradable starch-layered double hydroxide nanocomposites

Yi-Lin Chung, Hsi-Mei Lai *

Department of Agricultural Chemistry, National Taiwan University, No. 1, Roosevelt Rd., Sec. 4, Taipei 10617, Taiwan

ARTICLE INFO

Article history:
Received 2 September 2009
Received in revised form 1 December 2009
Accepted 11 December 2009
Available online 16 December 2009

Keywords:
Starch
Layered double hydroxide (LDH)
Synthetic clay
Nanocomposites

ABSTRACT

Well-dispersed starch-layered double hydroxide (LDH) nanocomposites were prepared by a newly developed approach of directly synthesizing the LDH in the starch dispersion. The approach involved a fast LDH nuclei precipitation followed by a hydrothermal treatment that simultaneously leached starches from the granules and aged the LDH nuclei. X-ray diffraction and transmission electron microscopy analyses showed that the LDH crystallites homogeneously dispersed in the acid-modified corn starch (AMS) matrix, whereas they tended to aggregate in the native normal corn starch (NCS) matrix. The LDH did not significantly influence the crystalline structure of starch molecules in the nanocomposites. The addition of LDH resulted in a pronounced phase separation in NCS, but not in AMS. With 10.47 wt.% of LDH, the AMS–LDH nanocomposites displayed unchanged transparency and moisture sensitivity, and an increase in modulus by as much as 37%. Our study revealed that lower-viscous starches produced by a proper acid modification can facilitate the dispersion of LDH and improve the modulus of nanocomposites.

1. Introduction

Plastic products prepared from synthetic polymers have already been widely utilized in diverse areas. These materials are not easily degradable and cause serious environmental problems. In recent years, bioplastics have raised a great interest because of an increased consciousness for sustainable development (Mooney, 2009; Queiroz & Collares-Queiroz, 2009; Zhao, Torley, & Halley, 2008). This concern has been translated into a demand for biodegradable products made of renewable raw materials. Among potential renewable materials (e.g., protein, polylactic acid, polyhydroxybutyrate) in eco-friendly markets, starches are considered relatively abundant and inexpensive biopolymers with good biodegradability. In the presence of plasticizers, starches can also be processed using conventional thermoplastic techniques. In spite of these advantages, starch-based materials are not yet widely commercialized, mostly due to their water sensitivity and inadequate mechanical properties (Follain, Joly, Dole, & Bliard, 2005). Developing new techniques to improve the properties of starch-based materials is thus in urgent need.

Nanocomposites are polymeric materials filled with dispersed particles with at least one dimension in nanometer range. They offer unique properties such as high modulus, low permeability, light weight, good thermal stability, and transparency (Giannelis, 1996; Paul & Robeson, 2008; Samir, Alloin, & Dufresne, 2005). Common nanofillers include clay, silica nanoparticles, carbon nanotubes, cellulose nanowhiskers, and graphene. Among these, clay has attracted considerable attention due to its availability, low cost, and significant mechanical enhancements. However, such enhancements can only be achieved when clay particles were well dispersed in a polymeric matrix (Crosby & Lee, 2007; Pavlidou & Papaspyrides, 2008). The good dispersion of clay particles maximizes the number of reinforcing elements for carrying an applied load. The tremendous interfacial area between the clay and the polymer matrix results in mechanical property improvements.

Most of the reported starch–clay nanocomposites suffer from poor dispersion, while the good dispersion of nanoparticles in matrix is required for obtaining high performance materials (Bagdi, Muller, & Pukanszky, 2006; Chiou et al., 2006; Pandey & Singh, 2005; Park, Lee, Park, Cho, & Ha, 2003; Park et al., 2002; Wilhelm, Sierakowski, Souza, & Wypych, 2003a, 2003b). To improve the dispersion, organic cations such as stearyl dihydroxyethyl ammonium chloride (Bagdi et al., 2006), distearyl dimethyl ammonium chloride (Bagdi et al., 2006) and quaternary ammonium-modified starches (Chivrac, Pollet, Schmutz, & Averous, 2008) were used to exchange with the sodium ions residing in the interlayer of pristine montmorillonite. The more the modifier is compatible with starch, the more it facilitates the clay dispersion (Chivrac et al., 2008). However, miscibility is still an issue and clay dispersion remains a challenge (Bagdi et al., 2006; Chiou et al., 2006; Park et al., 2002, 2003).

In this study, we present the preparation of well-dispersed starch–clay nanocomposites with two different kinds of starch:

* Corresponding author. Tel.: +886 2 33664816; fax: +886 2 23633123.
E-mail address: hmlai@ntu.edu.tw (H.-M. Lai).

0144-8617/$ - see front matter © 2009 Elsevier Ltd. All rights reserved.
doi:10.1016/j.carbpol.2009.12.020

native normal corn starch (NCS), and acid-modified normal corn starch (AMS). AMS is of interest because acid-modified starches showed a better film-forming ability than native starches (Chung & Lai, 2007). It was also hypothesized that the AMS slurry with lower viscosity is favorable for clay dispersion. LDH is a synthetic clay and compatible with biopolymers, such as DNA (Choy, Kwak, Park, Jeong, & Portier, 1999), polyaspartate (Whilton, Vickers, & Mann, 1997), alginic acid, pectin, κ-carrageenan, ι-carrageenan, and xanthan gum (Darder, Lopez-Blanco, Aranda, Leroux, & Ruiz-Hitzky, 2005; Darder, Ruiz, Aranda, Van Damme, & Ruiz-Hitzky, 2006). Well-dispersed starch–LDH nanocomposites were prepared by growing LDH crystallites in starch dispersions under hydrothermal treatment conditions. The LDH miscibility and dispersion from nanometer to micrometer scale were characterized using X-ray diffractometer (XRD), transmission electron microscopy (TEM), and optical light microscope. Furthermore, the mechanical properties, moisture adsorption, and transparency of starch–LDH nanocomposites were investigated. The findings will provide a novel and efficient strategy for the incorporation and homogeneous dispersion of clay in starch matrix.

2. Experimental

2.1. Materials

Native normal corn starch was purchased from Gu-Tong Foods Industrial Ltd. (Chia-Yi, Taiwan). The acid-modified corn starch was prepared by hydrolyzing native normal corn starch (137.5 g) with aqueous HCl (0.36%, 550 mL) at 45 °C for 33 h. The reaction was stopped by cooling down the reactants in an ice bath and neutralizing the reaction mixture with 1 M $NaHCO_3$. The suspension was then centrifuged at 4000*g* for 5 min. The residue was washed with 50% ethanol until free of chlorides and dried at 40 °C for 1 d. All reagents were analytical grade or higher and used as received.

2.2. Synthesis of starch–LDH nanocomposites

Corn starches (4.8 g) were suspended in 30 mL of mixed salt solutions containing $Mg(NO_3)_2{\cdot}6H_2O$ (0.075–0.3 M) and $Al(NO_3)_3{\cdot}9H_2O$ (0.025–0.1 M). To synthesize the LDH nuclei, the suspensions were quickly added 0.15 M NaOH (120 mL) with vigorous stirring under N_2 atmosphere, followed by stirring at 40 °C for 30 min. The precipitate was obtained by centrifugation at 10,000*g* for 5 min, washed twice with water (150 mL), and then dispersed in water (120 mL). After autoclaving at 100 °C for 16 h, the starch–LDH slurry was sheared in a homogenizer (Oster 10 Speed Blender, Florida, USA) at a high speed for 3 min. Starch–LDH slurry (25 g) was immediately poured into a Petri dish (i.d. 13.7 cm) and dried at 25 °C/53% RH for 9 h. The thickness of starch–LDH nanocomposites was ~50 μm. The mixed salts and NaOH solutions were prepared using decarbonated ultrapure water with a resistivity of 18.2 MΩ cm.

2.3. Chemical analysis of starch–LDH nanocomposites

The Mg and Al contents of samples were analyzed using an inductively coupled plasma atomic emission spectrometer (ICP-AES, PerkinElmer Opitma 2000, USA). Nanocomposites (40 mg) or LDH (5 mg) were dissolved in 1 mL of concentrated nitric acid and heated at 100 °C for 5 min. The digest was diluted, filtered (0.45 μm) and then injected into ICP-AES.

2.4. X-ray diffraction

Starch–LDH nanocomposites were conditioned at 25 °C/53% RH or 97% RH for 48 h before measurements. X-ray diffraction analysis was performed on a PANalytical X'Pert PRO diffractometer (Netherlands) with Cu Kα radiation (λ = 1.54 Å) operating at 45 kV and 40 mA. Scans were made from 5° to 40° (2θ) at a rate of 0.104°/s, a step of 0.008°, and time per step of 10.16 s. Relative B- and V_H-type crystallinities were calculated following a formula of Rindlav, Hulleman, and Gatenholm (1997) with some modifications: where A_{x-y} = the diffraction area from x to y degree. The denominator was modified

$$\text{Relative B- or } V_H - \text{type crystallinity}\,(\%) = \frac{A_{16-18^\circ}\,(\text{B type}) \text{ or } A_{21-22^\circ}\,(V_H \text{type})}{A_{8-40^\circ} - A_{9-13^\circ}} \times 100$$

by subtracting LDH diffraction area (A_{9-13°) from total diffraction area (A_{8-40°).

XRD analysis was also performed on a Geigerflex diffractometer (Regaku, Japan) with Cu Kα radiation operating at 35 kV and 15 mA. Scans for LDH powders were made from 4° to 40° (2θ) at a rate of 2°/min with a step of 0.1°. For NCS4 and AMS4, scans were made in the range of 2θ = 3–15° at a rate of 1°/min with a step of 0.05°.

2.5. Microstructure

Transmission electron microscopy was performed on a JOEL JEM-1230 electron microscope and operated at 100 kV. Nanocomposites were embedded in epoxy resin and sectioned (~100 nm). Specimens of LDH were prepared by dropping LDH suspensions onto a 200-mesh copper grid which coated with a carbon film.

Optical light microscope (ECLIPSE E600W POL, Nikon, Japan) was also used to examine the microstructure of nanocomposites.

2.6. Opacity

The opacity of starch–LDH nanocomposite was measured spectrophotometrically (Pharma Spec UV-1700, Shimadzu, Kyoto, Japan) and defined as the area under the absorbance spectrum between 400 and 800 nm divided by the sample thickness. The samples were conditioned at 25 °C/53% RH for 48 h before the measurements. At least five replicates were investigated on each sample.

2.7. Mechanical properties

A Texture analyzer *TA-XT2i* (Stable Micro System, Godalming, England) with 5 kg load cell in a tensile mode was used to measure Young's modulus, tensile strength, and elongation at break of sample strips (10 × 120 mm). Space between grips was 100 mm and grip speed was 0.8 mm/s. Samples were conditioned at 25 °C/53% RH for 48 h before testing. At least ten replicates were measured on each sample.

2.8. Moisture adsorption

The samples were dried in a chamber containing P_2O_5 for 72 h before being equilibrated at different relative humidity (RH). Different saturated salt solutions (LiCl, $MgCl_2$, $Mg(NO_3)_2$, NaCl, and K_2SO_4) were prepared in the individual sealed containers to create the specific relative humidity (11%, 33%, 53%, 75%, and 97% RH) at 25 °C. The moisture content was calculated from the mass increase of the dried sample after equilibration at a given RH condition. Moisture sorption determinations were duplicated.

2.9. Statistical analysis

The data were analyzed with SAS software (Version 8.2, SAS Institute Inc., Cary, NC). Duncan's multiple range tests were used to analyze the differences at the significance level $p < 0.05$ to compare the mean values across the treatments.

3. Results and discussion

3.1. Synthesis of starch–LDH nanocomposites

Preparation of starch–LDH nanocomposites involved two steps. In the first step, rapid addition of a suspension of starch with Mg^{2+} and Al^{3+} salts to an alkaline solution gave rise to a high amount of LDH nuclei. The co-precipitation of the two metallic salts resulted in LDH sheets (He et al., 2006). At the same time, some starch molecules leached from starch granules because of the high pH condition. Following precipitation of LDH nuclei, a hydrothermal treatment was performed to disrupt the granular structure of starch and completely leach starch molecules. This has been confirmed by the observations with optical light microscope. The well-dispersed LDH crystallites were supposed to grow and then be trapped between starch molecules during the hydrothermal treatment.

Elemental analysis of the starch–LDH nanocomposites confirmed the presence of LDH (Table 1). NCS1-4 and AMS1-4 were nanocomposites made from normal corn starch and acid-modified normal corn starch with different LDH contents. The Mg/Al molar ratios of NCS1-4 (1.93–1.96) were slightly higher than those of AMS1-4 (1.84–1.86). The general formula of LDH is $[M^{2+}_{1-x}M^{3+}_{x}(OH)_2]$-$(A^{m-}_{x/m})$-$nH_2O$. The chemical formulas of LDH in NCS1-4 and AMS1-4 were proposed to be $[M^{2+}_{0.66}M^{3+}_{0.34}(OH)_2]$-$(NO_3^-)_{0.34}$-$nH_2O$ and $[M^{2+}_{0.65}M^{3+}_{0.35}(OH)_2]$-$(NO_3^-)_{0.35}$-$nH_2O$, respectively. It has been previously reported that the x values of LDH were in the range of 0.1–0.5 (Khan & O'Hare, 2002). The x values of pure LDH, on the other hand, were between 0.2 and 0.33, which corresponds to the Mg/Al molar ratios of 2–4 (Weir, Moore, & Kydd, 1997). The x values that we detected were slightly above the range of 0.2–0.33. This may be attributed to the presence of other chemical compounds, such as in brucite ($Mg(OH)_2$) or gibbsite ($Al(OH)_3$), in the nanocomposites.

Fig. 1a is the TEM image of LDH prepared by the same procedure for synthesizing NCS4/AMS4. The LDH was in the form of well-shaped hexagons with a lateral size of 60 ± 18 nm. X-ray diffraction patterns of the LDH powders showed good crystallinity (Fig. 1b). According to the Joint Committee on Powder Diffraction Standards, the diffraction peaks at 11.55° (003), 23.26° (006), 34.76° (009) (012), 39.29° (015), 46.66° (018), 60.82° (110), 62.20° (113), 66.23° (116) represented LDH stacked in a rhombohedral structure.

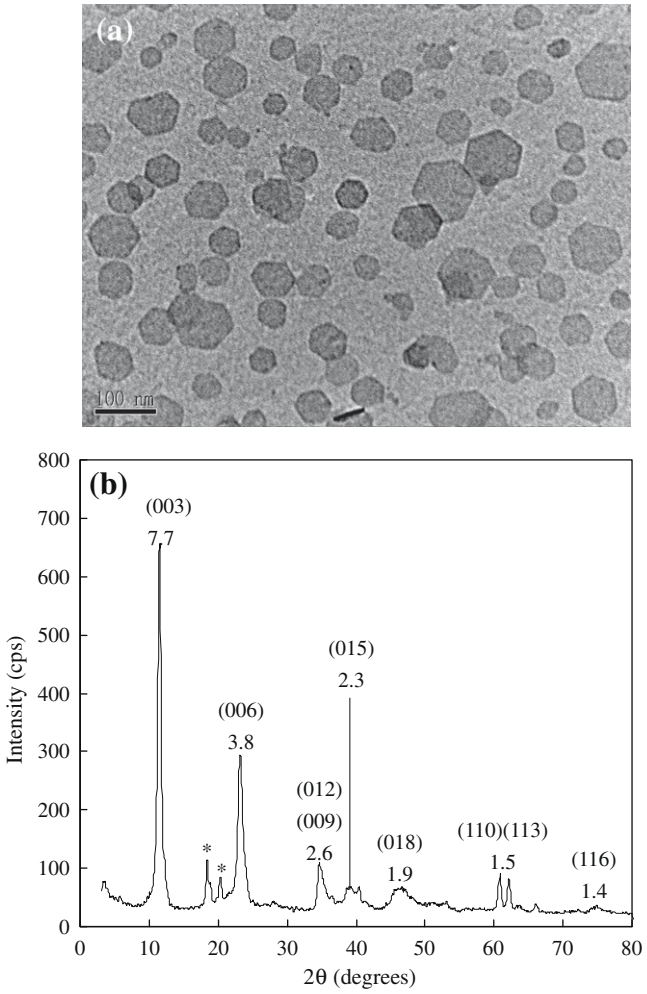

Fig. 1. (a) TEM image and (b) XRD pattern of LDH. The numbers indicated in the XRD pattern represent the d-spacing (Å) of LDH crystals. The diffraction peak (*) might result from gibbsite (0 0 2) and (2 0 0).

The basal spacing of LDH was 7.7 Å, similar to those reported elsewhere (Evans & Slade, 2006; Xu, Stevenson, Lu, & Lu, 2006). The impurity peaks shown in Fig. 1b came from crystals of $Al(OH)_3$; there were no diffraction peaks of $Mg(OH)_2$. Thus, the slightly low Mg/Al ratio of starch–LDH nanocomposites might be due to the increased concentration of aluminum, owing to the co-precipitation of LDH and traces of $Al(OH)_3$. Besides, the leaching of Mg^{2+} from the LDH sheets during the hydrothermal treatment also resulted in a low Mg/Al ratio (Boclair & Braterman, 1999). The esti-

Table 1
LDH contents and relative B-type crystallinities of NCS–LDH and AMS–LDH nanocomposites.

Sample	Mg%	Al%	Mg/Al molar ratio	LDH%[a] (db)	Relative B-type crystallinity (%)	
					53% RH	97% RH
NCS1	0	0	–	0	24.92 ± 0.31 a, A[b]	24.46 ± 0.16 b, A
NCS2	0.62	0.35	1.96	3.31 ± 1.16	22.53 ± 0.13 bc, A	25.25 ± 0.09 a, B
NCS3	0.94	0.53	1.94	5.08 ± 1.17	21.64 ± 0.66 c, A	25.48 ± 0.16 a, B
NCS4	2.16	1.24	1.93	11.66 ± 1.59	23.35 ± 0.81 b, A	23.20 ± 0.42 c, A
AMS1	0	0	–	0	23.35 ± 0.08 c, A	25.16 ± 0.50 ab, B
AMS2	0.42	0.25	1.84	2.66 ± 0.63	24.95 ± 0.06 a, A	25.49 ± 0.18 a, A
AMS3	1.41	0.84	1.86	7.60 ± 1.21	23.72 ± 0.00 b, A	22.86 ± 0.48 c, A
AMS4	1.96	1.18	1.84	10.47 ± 0.30	22.88 ± 0.16 d, A	24.34 ± 0.07 b, B

[a] LDH% = (Mg% in nanocomposites × weight of LDH)/(Mg% in LDH × weight of nanocomposites).
[b] Values followed by the different lowercase letters are significantly different at $p < 0.05$ within NCS–LDH and AMS–LDH nanocomposites under the same relative humidity. The different capital letters represent significant difference at $p < 0.05$ between 53% RH and 97% RH.

mated percentage of LDH in NCS1-4 and AMS1-4 are given in Table 1. The percentage of LDH of NCS2-4 and AMS2-4 were similar, but that of AMS3 (7.60 ± 1.21%) was slightly higher than that of NCS3 (5.08 ± 1.17%).

3.2. Structure of starch–LDH nanocomposites

In Fig. 2 the X-ray diffraction patterns of starch–LDH nanocomposites are presented. When LDH was synthesized in the starch slurry under hydrothermal treatment, the interlayer spacing of LDH crystallites remained at 7.7–7.9 Å (2θ = 11.2–11.6°) (Fig. 2a). The crystal size (t) perpendicular to (003) was calculated to be 55–58 Å using Scherrer's equation: $t = (0.9 \times \lambda)/((B - b) \times \cos\theta_B)$ where λ is 1.54 Å, and θ_B, B, and b are the angle of the diffraction peak, the width of the peak at half of its intensity, and the instrumental broadening, respectively (Cullity & Stock, 2001). This crystal size corresponded to approximately 7 layers of brucite-like sheets. Using the same calculation method, the pristine LDH (synthesized without starch) had 29 layers per stack and a thickness of 220 Å (Fig. 1). Therefore, the presence of starch during the synthesis of LDH effectively inhibited the stacking of clay sheets. Furthermore, the absence of the signal at low angle (Fig. 2b) indicated that there was no intercalated structure in the starch–LDH nanocomposites. This is because native normal corn starches are high molecular weight (1×10^6 to 10^8) polymers, composed of anhydroglucose units which are connected through α-(1 → 4) and α-(1 → 6)-linkages. These rigid structures make it difficult for starches to intercalate into the galleries between LDH sheets.

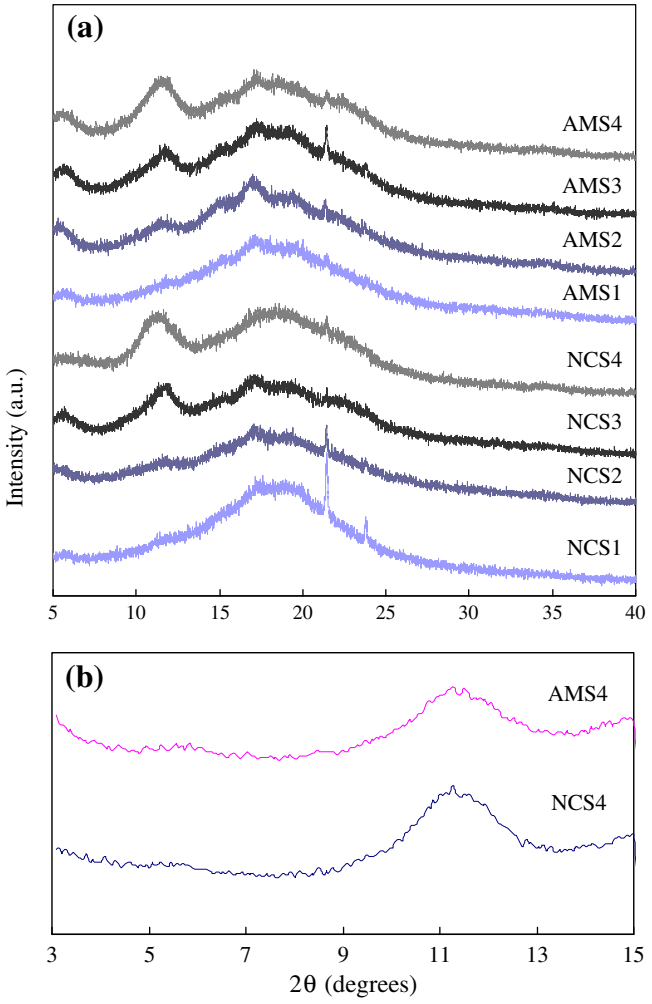

Fig. 2. (a) Wide-angle, and (b) small-angle XRD patterns of native normal corn starch (NCS), and acid-modified corn starch (AMS)–LDH nanocomposites equilibrated at 53% RH.

Starch–LDH nanocomposites containing various percentages of LDH exhibited the B-type X-ray diffraction patterns of starches with peaks at 2θ = 5.6°, 17° and 24° (Fig. 2a). The A-type crystalline structure, packed in a monoclinic unit cell with eight water molecules per unit cell (Imberty, Chanzy, Perez, Buleon, & Tran, 1988), of native normal corn starches was completely disrupted during the hydrothermal treatment (confirmed by the observations with optical light microscope). The dispersed starch molecules then recrystallized during drying process and resulted in a B-type crystalline structure. In B-type structure, the double helices, formed by branch chains of amylopectin and part of amylose, are packed in a hexagonal unit cell with 36–42 water molecules per unit cell (Imberty & Perez, 1988).

Table 1 gives the relative B-type crystallinities of starch–LDH nanocomposites after storage at intermediate (53%) and high (97%) relative humidity for 2 days. The relative B-type crystallinity of NCS2, NCS3, AMS1 and AMS4 was 1–4% higher at 97% RH than the samples stored at 53% RH. This is because the nanocomposites stored at the lower relative humidity, which adsorbed more water, were easier to recrystallize than those conditioned at the lower RH. NCS3 and AMS4 conditioned at 53% RH had the lowest relative B-type crystallinity, whereas the crystallinity of NCS4 and AMS3 was the lowest after equilibration at 97% RH.

The V_H-type diffraction pattern, recognized by an additional peak at 21.5° (2θ), is resulted from the single-helical structures, indicating the complexes formation of amylose and native lipids (Bader & Goritz, 1994). The V_H-type crystallinity of both NCS–LDH and AMS–LDH nanocomposites was similar (4–5%). It has been reported that the incorporation of clay into starch-based nanocomposites could restrain the crystallization behavior of biopolymers (Huang, Yu, & Ma, 2004; Huang, Yu, Ma, & Jin, 2005). However, the relative V_H-type crystallinity of starch–LDH nanocomposites did not significantly decrease with increasing the content of LDH. The interaction between starch and LDH in this system might not be strong enough to restrain the re-crystallization behavior effectively.

Fig. 3 shows TEM images of starch–LDH nanocomposites. The orientation of the LDH crystals in NCS and AMS showed no preference for lying on their basal crystal face (0 0 3) in any direction. That is expected as there was no strong shear force or squeezing flow from the casting process. The viscous starch–LDH slurry also prevented the LDH nanoparticle from lying on its basal face. The LDH was seen to possess an aggregated morphology in NCS4 (Fig. 3a and c), whereas they were almost individually dispersed in AMS4 (Fig. 3b and d). The LDH crystallites were 40–60 nm wide with the thickness of 5–10 nm, which is consistent with XRD data (55–58 Å).

The structure of the starch–LDH nanocomposites was also examined with an optical light microscopy (Fig. 4). It appeared that the bulk of NCS (Fig. 4a) and AMS (Fig. 4e) without LDH was phase-separated. The amylose- and amylopectin-rich phases were resulted from the incompatibility between amylose and amylopectin molecules (Rindlav-Westling & Gatenholm, 2003; Svegmark & Hermansson, 1991, 1993). The phase-separated structure was more pronounced in AMS films than in the NCS films since amylose retrograded quickly than did amylopectin. In the case of starch–LDH nanocomposites, the inhomogeneous structure in the NCS matrix was obvious with increasing in the percentage of LDH (Fig. 4b–d). On the other hand, the structure of AMS4 (Fig. 4h) with a higher percentage of LDH was much more homogeneous than was AMS1 (Fig. 4e). The mechanism is not known, but the results indicated that the changes in molecular weight and structure of the starch molecules significantly changed the interactions be-

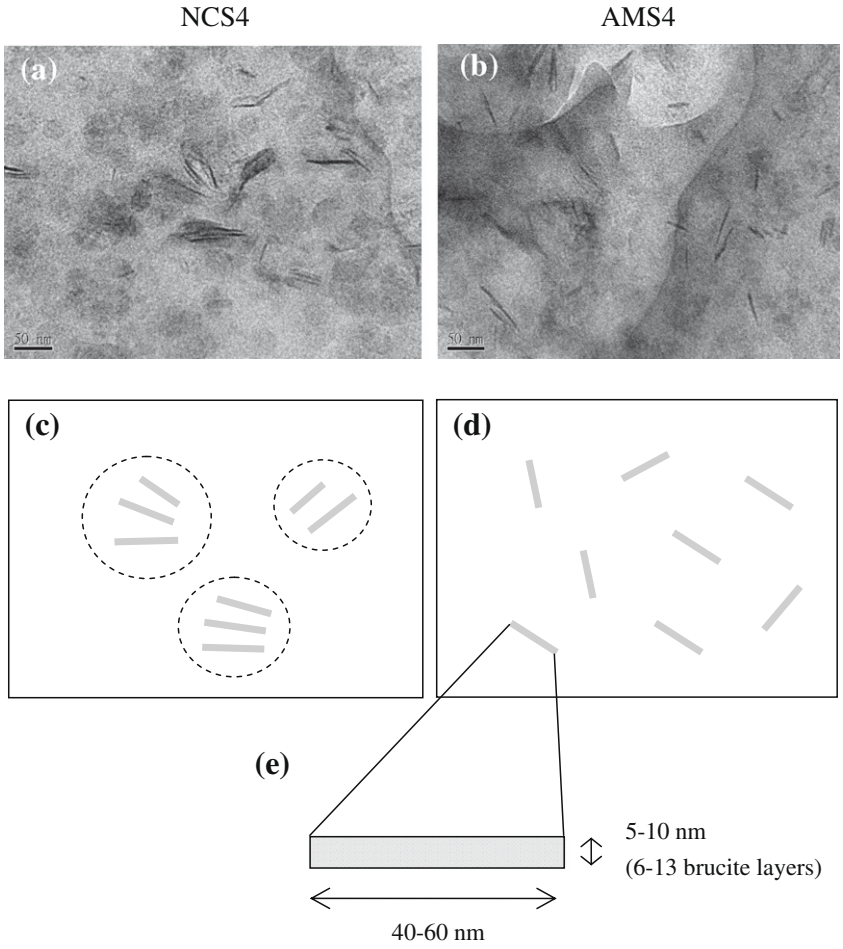

Fig. 3. (a and b) TEM images of starch–LDH nanocomposites and (c–e) schematic representations of LDH dispersion in starch matrix. (a and c) NCS4 and (b and d) AMS4. The scale bars on TEM images are 50 nm.

tween them and LDH and affected the structure of the resulting materials.

3.3. Properties of starch–LDH nanocomposites

The tensile properties of NCS–LDH and AMS–LDH nanocomposites with different percentages of LDH are given in Table 2. For samples without LDH, the Young's modulus and tensile strength of nanocomposites of native normal corn starch (NCS1) were greater than that of acid-modified corn starch (AMS1), but the elongation at break was decreased. This is expected since the molecular weight of starch decreased and the linear short chains increased after acid hydrolysis (Chung & Lai, 2006), causing AMS to be a relatively softer material. In theory, the well-dispersed nanoclays can constrain the surrounding polymers, decrease the mobility of matrix chains, and further result in the enhancement in the mechanical properties of materials (Crosby & Lee, 2007). However, the tensile strength and elongation at break of NCS-based materials decreased with increasing in the content of LDH (NCS1 > NCS2 > NCS3 > NCS4). The property enhancement is not only depended on the type and amount of nanoclay, but also on the structure of the polymer matrix. As indicated by Fig. 4a–d, the phase separation of nanocomposites with a high LDH content might destroy the integrity of the NCS nanocomposite structure. Thus, their mechanical properties did not show the same degree of enhancement as found in other nanocomposite systems.

For AMS-based nanocomposites, the Young's modulus increased with increasing in the concentration of LDH (AMS4 > AMS3 > AMS2 > AMS1) (Table 2). The increase was a consequence of the incorporation of LDH, which increased the stiffness as well as reduced the phase separation of starch matrix. The Young's modulus of AMS4 increased 37%, compared to the unfilled starch matrix. The tensile strength of AMS–LDH nanocomposites did not increase with increasing in the loading of LDH. This indicated that the incorporation of LDH, which increased the stiffness of the starch matrix at a low strain, did not change its stiffness at a high strain. At a higher LDH loading (10.84%), the elongation at break of AMS4 dropped to 1.81%. It is speculated that, easier of LDH crystallites associate with each others and thus higher amount of aggregated LDH formed when more LDH existed, leading to a decreased elongation property.

Fig. 5a shows the opacity of the NCS–LDH and AMS–LDH nanocomposites. The opacity of NCS and AMS samples without LDH was similar ($\sim 40 \times 10^{-5}$ AU). When increasing the loading of LDH, the opacity of NCS–LDH nanocomposites increased significantly ($\sim 100 \times 10^{-5}$ AU). However, the AMS–LDH nanocomposites were uniformly translucent between 0% and 10% of LDH loadings (Fig. 5b). This suggested that the dispersion and miscibility of the nanophases in AMS were much better than those in the NCS matrix.

Because the properties of starch-based materials are easily influenced by relative humidity, moisture adsorption curves are used to evaluate the storage properties of starch–LDH nanocomposites (Fig. 6). The moisture content of samples slowly increased with increasing in the equilibrium relative humidity up to 70%, above that a steep raise in moisture content was observed. The

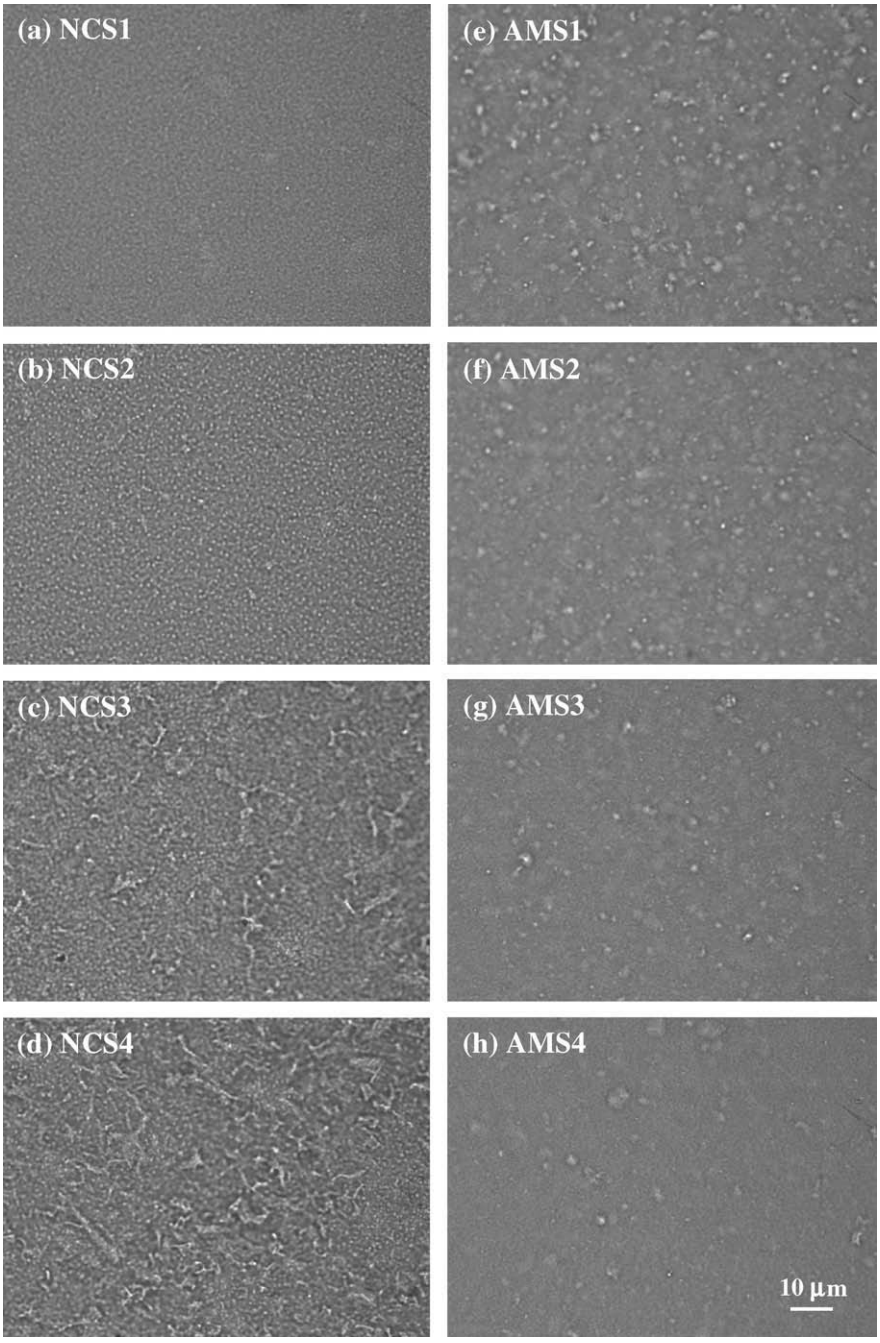

Fig. 4. Optical images of (a–d) NCS–LDH and (e–h) AMS–LDH nanocomposites.

Table 2
Mechanical properties of NCS–LDH and AMS–LDH nanocomposites. The samples were conditioned at 53% RH before measurement.

Sample	Young's modulus (MPa)	Tensile strength (MPa)	Elongation at break (%)
NCS1	2805 ± 305 a[a]	35.73 ± 3.92 a	2.77 ± 0.73 a
NCS2	2519 ± 258 b	31.13 ± 2.25 b	3.14 ± 1.38 a
NCS3	2734 ± 267 a	30.43 ± 2.74 b	2.58 ± 0.95 a
NCS4	2841 ± 177 a	27.51 ± 2.84 c	1.80 ± 0.66 b
AMS1	2424 ± 168 a	31.12 ± 2.48 a	3.55 ± 0.82 a
AMS2	2701 ± 152 b	33.89 ± 2.32 a	3.52 ± 0.99 a
AMS3	2734 ± 259 b	32.51 ± 3.50 a	3.53 ± 1.10 a
AMS4	3316 ± 363 c	31.85 ± 3.30 a	1.81 ± 0.54 b

[a] Values followed by the different letters are significantly different at $p < 0.05$ within NCS–LDH and AMS–LDH nanocomposites.

moisture content of nanocomposites did not significantly changes when LDH was added in both NCS and AMS systems. This revealed that the water adsorption of starch–LDH nanocomposites during storage is dominated by the starch matrix because of the relatively strong hydrophilicity of starch molecules.

4. Conclusions

Starch–clay composites have been generally prepared by blending the two components in suspensions or in extruders. We presented a newly developed approach towards the synthesis of starch–clay nanocomposites. Using this method, LDH nanoparticles can be embedded in a starch matrix by directly synthesizing the LDH in the starch dispersion. During the reaction, the LDH

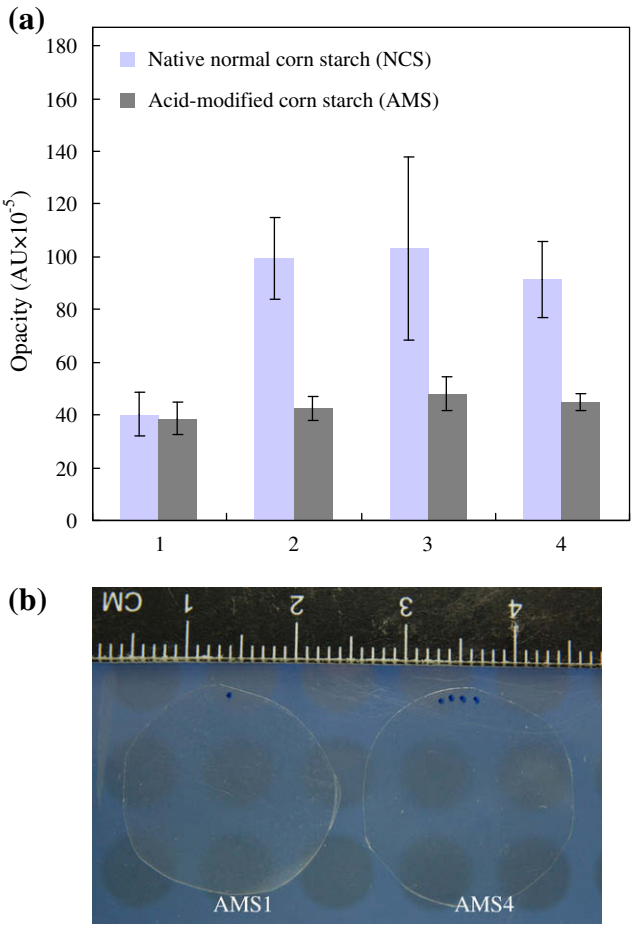

Fig. 5. (a) Opacity of NCS–LDH and AMS–LDH nanocomposites and (b) photos of AMS1 and AMS4.

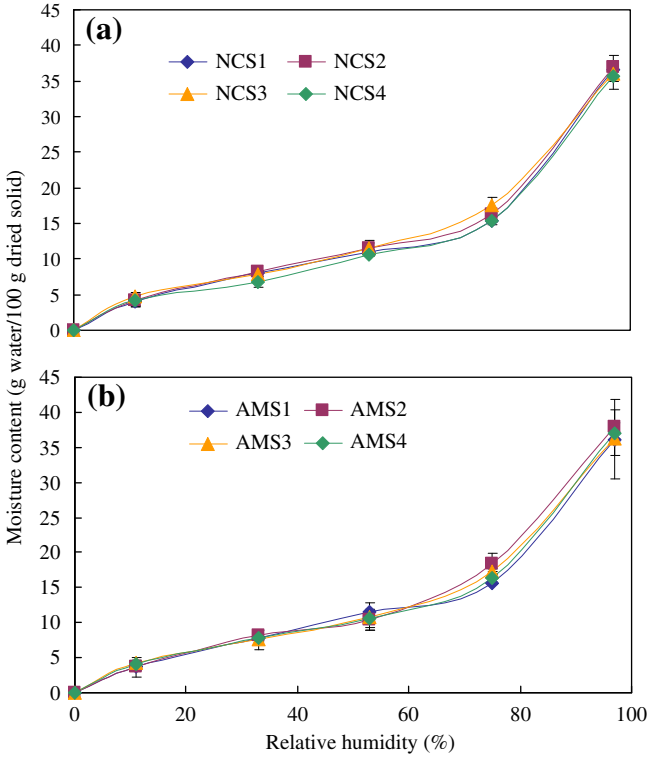

Fig. 6. Moisture adsorption of NCS–LDH and AMS–LDH nanocomposites.

nuclei were first precipitated in partially gelatinized starch dispersion, and then gradually aged in the dispersed starch under a hydrothermal condition. The acid modification process reduced the molecular weight and pasting viscosity of the starch, facilitating the dispersion of LDH crystallites in the nanocomposite. The addition of LDH in acid-modified corn starch matrix was proved to be effective in improving the modulus of starch–clay nanocomposites without sacrificing their transparency and moisture sensitivity.

Acknowledgement

This work was supported by the Grant NSC-96-2313-B-002-048-MY2 from the National Science Council, Taipei, Taiwan.

References

Bader, H., & Goritz, D. (1994). Investigations on high amylose corn starch films. Part I. Wide-angle X-ray scattering (WAXS). *Starch/Staerke, 46*, 229–232.
Bagdi, K., Muller, P., & Pukanszky, B. (2006). Thermoplastic starch/layered silicate composites: Structure, intercalation, properties. *Composite Interfaces, 13*, 1–17.
Boclair, J. W., & Braterman, P. S. (1999). Layered double hydroxide stability. 1. Relative stabilities of layered double hydroxides and their simple counterparts. *Chemistry of Materials, 11*, 298–302.
Chiou, B. S., Yee, E., Wood, D., Shey, J., Glenn, G., & Orts, W. (2006). Effects of processing conditions on nanoclay dispersion in starch–clay nanocomposites. *Cereal Chemistry, 83*, 300–305.
Chivrac, F., Pollet, E., Schmutz, M., & Averous, L. (2008). New approach to elaborate exfoliated starch-based nanobiocomposites. *Biomacromolecules, 9*, 896–900.
Choy, J. H., Kwak, S. Y., Park, J. S., Jeong, Y. J., & Portier, J. (1999). Intercalative nanohybrids of nucleoside monophosphates and DNA in layered metal hydroxide. *Journal of the American Chemical Society, 121*, 1399–1400.
Chung, Y. L., & Lai, H. M. (2006). Molecular and granular characteristics of corn starch modified by HCl–methanol at different temperatures. *Carbohydrate Polymers, 63*, 527–534.
Chung, Y. L., & Lai, H. M. (2007). Properties of cast films made of HCl–methanol modified corn starch. *Starch/Staerke, 59*, 583–592.
Crosby, A. J., & Lee, J. Y. (2007). Polymer nanocomposites: The "nano" effect on mechanical properties. *Polymer Reviews, 47*, 217–229.
Cullity, B. D., & Stock, S. R. (2001). *Elements of X-ray diffraction*. New Jersey: Prentice Hall Inc.
Darder, M., Lopez-Blanco, M., Aranda, P., Leroux, F., & Ruiz-Hitzky, E. (2005). Bionanocomposites based on layered double hydroxides. *Chemistry of Materials, 17*, 1969–1977.
Darder, M., Ruiz, A. I., Aranda, P., Van Damme, H., & Ruiz-Hitzky, E. (2006). Bionanohybrids based on layered inorganic solids: Gelatin nanocomposites. *Current Nanoscience, 2*, 231–241.
Evans, D. G., & Slade, R. C. (2006). Structural aspects of layered double hydroxides. *Structure & Bonding, 119*, 1–87.
Follain, N., Joly, C., Dole, P., & Bliard, C. (2005). Mechanical properties of starch-based materials. I. Short review and complementary experimental analysis. *Journal of Applied Polymer Science, 97*, 1783–1794.
Giannelis, E. P. (1996). Polymer layered silicate nanocomposites. *Advanced Materials, 8*, 29–35.
He, J., Wei, M., Li, B., Kang, Y., Evans, D. G., & Duan, X. (2006). Preparation of layered double hydroxides. *Structure & Bonding, 119*, 89–119.
Huang, M. F., Yu, J. G., & Ma, X. F. (2004). Studies on the properties of montmorillonite-reinforced thermoplastic starch composites. *Polymer, 45*, 7017–7023.
Huang, M. F., Yu, J. G., Ma, X. F., & Jin, P. (2005). High performance biodegradable thermoplastic starch-EMMT nanoplastics. *Polymer, 46*, 3157–3162.
Imberty, A., Chanzy, H., Perez, S., Buleon, A., & Tran, V. (1988). The double-helical nature of the crystalline part of A-starch. *Journal of Molecular Biology, 201*, 365–378.
Imberty, A., & Perez, S. (1988). A revisit to the three dimensional structure of B-type starch. *Biopolymers, 27*, 1205–1221.
Khan, A. I., & O'Hare, D. (2002). Intercalation chemistry of layered double hydroxides: Recent developments and applications. *Journal of Materials Chemistry, 12*, 3191–3198.
Mooney, B. P. (2009). The second green revolution? Production of plant-based biodegradable plastics. *Biochemical Journal, 418*, 219–232.
Pandey, J. K., & Singh, R. P. (2005). Green nanocomposites from renewable resources: Effect of plasticizer on the structure and material properties of clay-filled starch. *Starch/Starke, 57*, 8–15.
Park, H. M., Lee, W. K., Park, C. Y., Cho, W. J., & Ha, C. S. (2003). Environmentally friendly polymer hybrids. Part I. Mechanical, thermal, and barrier properties of thermoplastic starch/clay nanocomposites. *Journal of Materials Science, 38*, 909–915.
Park, H. M., Li, X., Jin, C. Z., Park, C. Y., Cho, W. J., & Ha, C. S. (2002). Preparation and properties of biodegradable thermoplastic starch/clay hybrids. *Macromolecular Materials and Engineering, 287*, 553–558.

Paul, D. R., & Robeson, L. M. (2008). Polymer nanotechnology: Nanocomposites. *Polymer, 49*, 3187–3204.
Pavlidou, S., & Papaspyrides, C. D. (2008). A review on polymer-layered silicate nanocomposites. *Progress in Polymer Science, 33*, 1119–1198.
Queiroz, A. U. B., & Collares-Queiroz, F. P. (2009). Innovation and industrial trends in bioplastics. *Journal of Macromolecular Science, Part C: Polymer Reviews, 49*, 65–78.
Rindlav, A., Hulleman, S. H. D., & Gatenholm, P. (1997). Formation of starch films with varying crystallinity. *Carbohydrate Polymers, 34*, 25–30.
Rindlav-Westling, A., & Gatenholm, P. (2003). Surface composition and morphology of starch, amylose, and amylopectin films. *Biomacromolecules, 4*, 66–172.
Samir, M. A. S. A., Alloin, F., & Dufresne, A. (2005). Review of recent research into cellulose whiskers, their properties and their application in nanocomposite field. *Biomacromolecules, 6*, 612–626.
Svegmark, K., & Hermansson, A. M. (1991). Distribution of amylose and amylopectin in potato starch pastes – Effects of heating and shearing. *Food Structure, 10*, 117–129.
Svegmark, K., & Hermansson, A. M. (1993). Microstructure and rheological properties of composites of potato starch granules and amylose – A comparison of observed and predicted structures. *Food Structure, 12*, 181–193.
Weir, M. R., Moore, J., & Kydd, R. A. (1997). Effects of pH and Mg:Ga ratio on the synthesis of gallium-containing layered double hydroxides and their polyoxometalate anion exchange products. *Chemistry of Materials, 9*, 1686–1690.
Whilton, N. T., Vickers, P. J., & Mann, S. (1997). Bioinorganic clays: Synthesis and characterization of amino- and poly-amino acid intercalated layered double hydroxides. *Journal of Materials Chemistry, 7*, 1623–1629.
Wilhelm, H. M., Sierakowski, M. R., Souza, G. P., & Wypych, F. (2003a). The influence of layered compounds on the properties of starch/layered compound composites. *Polymer International, 52*, 1035–1044.
Wilhelm, H. M., Sierakowski, M. R., Souza, G. P., & Wypych, F. (2003b). Starch films reinforced with mineral clay. *Carbohydrate Chemistry, 52*, 101–110.
Xu, Z. P., Stevenson, G., Lu, C. Q., & Lu, G. Q. (2006). Dispersion and size control of layered double hydroxide nanoparticles in aqueous solutions. *Journal of Physical Chemistry B, 110*, 16923–16929.
Zhao, R., Torley, P., & Halley, P. J. (2008). Emerging biodegradable materials: Starch- and protein-based bio-composites. *Journal of Materials Science, 43*, 3058–3071.